Novel coumarin-nucleobase hybrids with potential anticancer activity: Synthesis, *in-vitro* cell-based evaluation, and molecular docking

Maiara Correa de Moraes[1,2], Rafaele Frassini[1], Mariana Roesch-Ely[1], Favero Reisdorfer de Paula[3] and Thiago Barcellos*[1]

[1] Universidade de Caxias do Sul, Francisco Getúlio Vargas St., 1130, 95070-560, Caxias do Sul, RS, Brazil.
[2] Instituto Federal de Educação, Ciência e Tecnologia do Rio Grande do Sul – Campus Caxias do Sul, Avelino Antônio de Souza, 1730, 95043-700, Caxias do Sul, RS, Brazil.
[3] Laboratório de Desenvolvimento e Controle de Qualidade em Medicamentos, Universidade Federal do Pampa, Campus Uruguaiana, BR 472, Km 592, 97508-000, Uruguaiana, RS, Brazil.
Corresponding author e-mail: thiago.barcellos@ucs.br

Abstract

A new series of compounds planned by molecular hybridization of the nucleobases uracil and thymine, or the xanthine theobromine, with coumarins, and linked through 1,2,3-triazole heterocycles were evaluated for their *in vitro* anticancer activity against the human tumor cell lines: colon carcinoma (HCT116), laryngeal tumor cells (Hep-2), and lung carcinoma cells (A549). The hybrid compound 7a exhibited better activity in the series, showing an IC_{50} of 24.19 ± 1.39 μM against the HCT116 cells, with a selectivity index (SI) of 6, when compared to the cytotoxicity against the non-tumor cell line HaCat. Molecular docking studies were performed on all active compounds and suggested that the synthesized compounds possess a high affinity to DNA Topoisomerase-1 protein, supporting their antitumor activity. The *in silico* toxicity prediction studies suggest that the compounds present a low risk of causing theoretical mutagenic and tumorigenic effects. These findings indicate that the molecular hybridization from natural derivative molecules is an interesting approach to seek new antitumor candidates.

Keywords: Molecular hybridization, coumarin, nucleobases, anticancer, molecular docking.

1. Introduction

One of the key challenges in medicinal chemistry is the development of more effective, selective and safer compounds for the treatment of known and new pathologies (Lombardino & Lowe, 2004). Even though there are almost infinite possibilities of novel chemical structures wanting for their bioactive properties evaluation, the molecular hybridization of known bioactive entities can be used as an alternative approach to optimize the process. Molecular hybridization involves the rational design and association of two or more pharmacophores into a single molecule, aiming at new molecular entities that allow: multiple biological activities, modified selectivity profiles, different or dual modes of action, and reduced undesired side effects (Claudio Viegas-Junior, Eliezer J. Barreiro & Carlos Alberto Manssour Fraga, 2007; Kerru et al., 2017; Ivasiv et al., 2019; Shalini & Kumar, 2021).

Coumarin and its natural and synthetic derivatives are a remarkable example of naturally based occurring heterocycle which presents an extensive range of pharmacological activities, including antibacterial (Kraljević et al., 2016), antitubercular (Reddy, Hosamani & Devarajegowda, 2015), sedative-hypnotic (Gomha et al., 2020), antioxidante (Salar et al., 2016), anti-inflammatory (Simijonović et al., 2018), anticoagulant (Popov Aleksandrov et al., 2018), antileishmanial (Gonçalves et al., 2020), and anticancer (Thakur, Singla & Jaitak, 2015; Emami & Dadashpour, 2015; Dandriyal et al., 2016; Gomha, Abdel-aziz & El-Reedy, 2018; Akkol et al., 2020).

The *2H*-chromen-2-one core is considered a privileged structure due to its rigid and conjugated structure. The aromatic ring allows a series of hydrophobic, π–π, CH–π, and cation–π interactions, and the two oxygen atoms in the lactone ring can also hydrogen-bond with amino acid residues in different classes of enzymes and receptors (Torres et al., 2016). The relevant pharmacological profile of the *H*-chromen-2-one nucleus is illustrated with its presence in the main backbone of approved drugs such as warfarin (anticoagulant), carbochromen (vasodilator), and novobin (antibiotic) (Singh et al., 2019). Regarding the molecular hybridization strategy, coumarins have also been employed along with diverse bioactive compounds (Sandhu et al., 2014; Kerru et al., 2017; Singh et al., 2019; Zhang & Xu, 2019).

Pyrimidine and derivatives are also a significant and widespread class of nitrogen-containing heterocycles that are an integral part of DNA and RNA building blocks. They play an essential role in the biological process, and consequently, have considerable chemical and

pharmacological importance. The 5-fluorouracil (5-FU) is an example of pyrimidine derivative that has been used in cancer treatment. 5-FU, such as other pyrimidine derivatives, act as antagonists in the biosynthetic pathways of pyrimidine nucleobases (Gazivoda Kraljević et al., 2014) competing for the same binding sites of naturally occurring compounds (Accetta et al., 2009).

1,2,3-Triazoles have been frequently used as an attractive binding unit (linker) between the pharmacophoric units (Ivasiv et al., 2019). The 1,2,3-triazole moiety is easily achieved through the dipolar cycloaddition between azides and alkynes (Krištafor et al., 2015; Deshmukh et al., 2019) and also presents several biological activities, which include antibacterial (Gao et al., 2019), antifungal (Shalini et al., 2011), and anticancer (Xu, Zhao & Liu, 2019). It is also metabolically stable and capable of forming hydrogen bonds, which could be favorable in binding biomolecular targets (Kraljević et al., 2016).

Coumarin and uracil derivatives conjugated to 1,2,3-triazoles have been reported in the literature and evaluated as possible anticancer agents. For instance, coumarin-chalcone hybrids linked by the 1,2,3-triazole ring were synthesized and evaluated as anticancer and antimalarial agents (Pingaew et al., 2014). The example A (Figure 1) showed antiproliferative activity against human acute T lymphoblastic leukemia cell lines (MOLT-3) with an IC_{50} of 0.53 µM.

An example of pyrimidine derivative employed in the molecular hybridization strategy is the uracil-isatin conjugates hybridized via the 1,2,3-triazole bridge (Kumar et al., 2012). Among the series prepared in this study, compound B (Figure 1) showed considerable selectivity for the human prostate cancer cell line (DU145) with an IC_{50} of 13.9 µM.

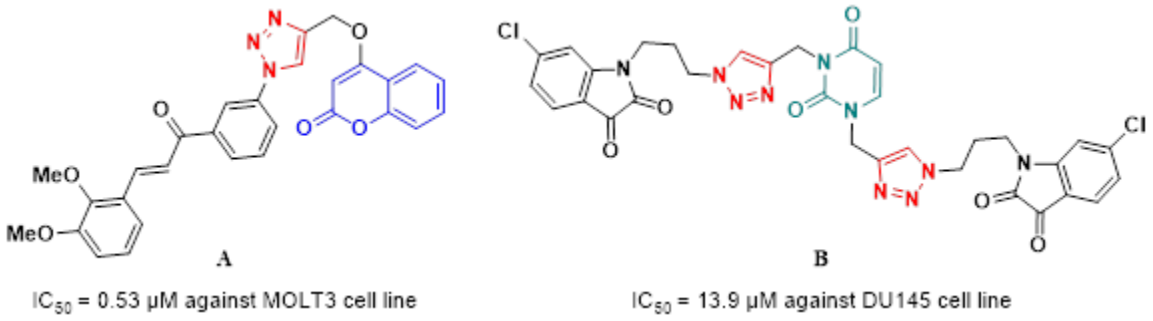

Figure 1. Representative examples of biologically active coumarin and uracil-containing compounds hybridized through the 1,2,3-triazole heterocycle.

Considering the pharmacological relevance of the coumarin and pyrimidine derivatives, in this work we explored their molecular hybridization linked by a triazole unit aiming to integrate their pharmacological properties. Thus, we investigate the potential anticancer activities of the novel coumarin-nucleobase hybrids against three human cell lines: colon carcinoma (HCT116), laryngeal tumor cells (Hep-2), and lung carcinoma cells (A549), and one non-tumor cell line, namely HaCat (human keratinocyte), by the colorimetric MTT assay.

2. Material and methods

2.1. Materials and instrumentation

All reagents and solvents used were purchased from commercial suppliers (Sigma-Aldrich®, São Paulo, Brazil) and used without further purification. The NMR experiments were performed on a Fourier 300 FT-NMR spectrometer (Bruker Daltonics, Bremen, German; 7.05 Tesla, 300 MHz for the ^{1}H nucleus and 75 MHz for the ^{13}C nucleus). The chemical shifts (δ) are expressed in part per million (ppm), and the coupling constants reported in Hz. The spectra were acquired at a temperature of 293 K, using 5 mm quartz tubes. For the NMR data acquisition and processing, the TopSpin™ software (Bruker) was used. The high-resolution electrospray ionization mass spectrometry (ESI-QTOF) analyses were performed on a micrOTOF-Q II instrument (Bruker Daltonics, Billerica, MA, USA) in positive mode, under the following conditions: capillary and cone voltages were set to +3500 V and +40 V, respectively, with a de-solvation temperature of 200 °C. The samples were solubilized in HPLC-grade methanol, containing 0.1% formic acid, and injected into the ESI source by means of a syringe pump at a flow rate of 5.0 μL min 1. Melting points were recorded on a capillary melting point apparatus (Fisatom, model 431, São Paulo, Brazil), with a measurement range from 50 °C to 350 °C and are uncorrected.

2.2. General procedure for the preparation of the 4-(chloromethyl)-coumarins 3a,b

Phenol (**1a** or **1b**) (5 mmol), ethyl 4-chloroacetoacetate (7.5 mmol), and sulfamic acid (10 mol%, 0.0485 g) were added to a 30 mL glass vial and tightly sealed with Teflon cap. The reaction mixture was heated at 100 °C, for 20 min (**1a**) or 6 h (**1b**). After, the reaction mixture was cooled to room temperature and dissolved in 25 mL of hot ethanol, filtered, and poured into an ice-water mixture (100 mL). The precipitate that formed was filtered and recrystallized from ethanol.

2.2.1. 4-(chloromethyl)-5,7-dihydroxy-2H-chromen-2-one (**3a**): white solid (970 mg, 86%); mp 231-233 ºC (lit.(Abbasi et al., 2017) 240-242 °C); ^{1}H NMR (300 MHz, acetone-d_6) δ 5.06 (d, *J* 1.2 Hz, 2H), 6.27 (t, *J* 1.2 Hz, 1H), 6.32 (d, *J* 2.4 Hz, 1H), 6.38 (d, *J* 2.4 Hz, 1H), 9.34 (s, 1H, OH), 9.85 (s, 1H, OH); ^{13}C NMR (75 MHz, DMSO-d_6) δ 45.10, 94.89, 99.32, 99.88, 108.85, 152.14, 156.59, 157.25, 160.19, 161.63; HRMS (ESI+) *m/z* calcd. for $C_{10}H_8ClO_4$ $[M+H]^+$: 227.0105, found: 227.0101.

2.2.2. 4-(chloromethyl)-2H-benzo[h]chromen-2-one (**3b**): light brown solid (850 mg, 70%); mp 154-156 ºC (lit.(Abbasi et al., 2017) 159-161 °C); ^{1}H NMR (300 MHz, DMSO-d_6) δ 5.12 (s, 2H, CH_2), 6.79 (s, 1H, CH), 7.76-7.69 (m, 2H), 7.91–7.83 (m, 2H), 8.06-8.03 (m, 1H), 8.37-8.34 (m, 1H); ^{13}C NMR (75 MHz, DMSO-d_6) δ 41.66, 112.78, 114.85, 120.89, 121.61, 122.23, 124.07, 127.53, 127.98, 128.97, 134.36, 150.32, 151.44, 159.52; HRMS (ESI+) *m/z* calcd. for $C_{14}H_{10}ClO_2$ $[M+H]^+$: 245.0363, found: 245.0369.

2.3. General procedure for the preparation of 4-(azidomethyl)-coumarins (4a,b)

In a 50 mL round-bottomed flask equipped with a magnetic stirrer, 4-(chloromethyl)-coumarins **3a**,**b** (2 mmol) was taken in 4 mL of acetone. After, a solution of sodium azide (2.4 mmol) in 0.6 mL of water was added dropwise with a continuous stirring, which was kept for an additional 10 h at 30 °C. The reaction mixture was poured into an ice-water. The precipitate that formed was filtered and recrystallized from ethanol (Naik et al., 2012).

2.3.1. 4-(azidomethyl)-5,7-dihydroxy-2H-chromen-2-one (**4a**): white solid (414 mg, 89%); mp 215-217 ºC (lit.(Ye et al., 2014) 220-221 °C); ^{1}H NMR (300 MHz, DMSO-d_6) δ 4.87 (d, *J* 1.1 Hz, 2H, CH_2), 6.05 (t, *J* 1.1 Hz, 1H, CH), 6.21 (d, *J* 2.4 Hz, 1H), 6.27 (d, *J* 2.4 Hz, 1H), 10.42 (s, 1H, OH), 10.88 (s, 1H, OH); ^{13}C NMR (75 MHz, DMSO-d_6) δ 52.79, 94.82, 99.11, 100.07, 106.76, 151.76, 156.52, 157.31, 160.09, 161.56; HRMS (ESI+) *m/z* calcd. for $C_{10}H_7N_3O_4Na$ $[M+Na]^+$: 256.0328, found: 256.0325.

2.3.2. 4-(azidomethyl)-2H-benzo[h]chromen-2-one (**4b**): light brown solid (431 mg, 86%); mp 136-138 ºC (lit.(Kusanur et al., 2010) 131 °C); ^{1}H NMR (300 MHz, DMSO-d_6) δ 4.97 (s, 2H, CH_2), 6.63 (s, 1H, CH), 7.76-7.70 (m, 3H), 7.88 (d, *J* 8.4 Hz 1H), 8.06-8.04 (m, 1H), 8.38-8.35 (m, 1H);

^{13}C NMR (75 MHz, DMSO-d_6) δ 49.97, 112.81, 112.92, 120.45, 121.59, 122.15, 124.14, 127.51, 127.97, 128.90, 134.33, 150.05, 150.79, 159.44; HRMS (ESI+) *m/z* calcd. for $C_{14}H_{10}N_3O_2$ $[M+H]^+$: 252.0767, found: 252.0762.

2.4. General procedure for monopropargylation of uracil and thymine. Synthesis of 6a and 6b.

In a 50 mL round-bottomed flask, equipped with a magnetic stirrer, uracil (**5a**, 0.560 g, 5 mmol) or thymine (**5b**, 0.631 g, 5 mmol) was suspended in dry acetonitrile (15 mL), *N,O*-bis-(trimethylsilyl)acetamide (BSA, 3.06 mL, 12.5 mmol) was added, and the mixture stirred until a clear solution was obtained. Subsequently, propargyl bromide (80 wt.% in toluene, 0.615 mL, 6.9 mmol) was added dropwise and the reaction mixture was heated at 45 °C for 72 h. The acetonitrile was evaporated under vacuum and the residue was treated with saturated aqueous NH_4Cl solution (15 mL) and extracted with CH_2Cl_2. The organic phase was dried with anhydrous Na_2SO_4 and concentrated under vacuum. The crude product was purified by recrystallization from CH_2Cl_2/hexane (1:2 v/v).

2.4.1. 1-(prop-2-yn-1-yl)pyrimidine-2,4(1H,3H)-dione (**6a**): white solid (465 mg, 62%); mp 153-155 ºC (lit.(González-Olvera et al., 2013) 169-170 °C); ^{1}H NMR (300 MHz, DMSO-d_6) δ 3.42 (t, *J* 2.4 Hz, 1H), 4.50 (d, *J* 2.4 Hz, 2H), 5.61 (d, *J* 7.8 Hz 1H), 7.69 (d, *J* 7.8 Hz 1H), 11.38 (br, 1H, NH); ^{13}C NMR (75 MHz, DMSO-d_6) δ 36.67, 75.89, 78.51, 101.71, 144.57, 150.43, 163.62; HRMS (ESI+) *m/z* calcd. for $C_7H_7N_2O_2$ $[M+H]^+$: 151.0502, found: 151.0507.

2.4.2. 5-methyl-1-(prop-2-yn-1-yl)pyrimidine-2,4(1H,3H)-dione (**6b**): white solid (620 mg, 76%); mp 150-152 ºC (lit.(González-Olvera et al., 2013) 155-157 °C); ^{1}H NMR (300 MHz, DMSO-d_6) δ 1.76 (d, *J* 1.0 Hz, 3H), 3.40 (t, *J* 2.4 Hz, 1H), 4.46 (d, *J* 2.4 Hz, 2H), 7.56 (d, *J* 1.0 Hz, 1H), 11.38 (br, 1H, NH); ^{13}C NMR (75 MHz, DMSO-d_6) δ 11.98, 36.36, 75.69, 78.70, 109.43, 140.19, 150.40, 164.19; HRMS (ESI+) *m/z* calcd. for $C_8H_9N_2O_2$ $[M+H]^+$: 165.0658, found: 165.0654.

2.5. Synthesis of 1,3-di(prop-2-yn-1-yl)pyrimidine-2,4(1*H*,3*H*)-dione (6c)

In a 50 mL round-bottomed flask, equipped with a magnetic stirrer, were added a suspension of potassium carbonate (4 mmol, 0.552 g) in anhydrous DMF (10 mL), and uracil (1

mmol, 0.112 g). The mixture was stirred for one hour, at room temperature. After, propargyl bromide (80 wt.% in toluene, 0.212 mL, 2.4 mmol) was added, and the reactions mixture was kept under stirring for 24 hours at room temperature. After the reaction completion, the mixture was treated with brine (20 mL) and extracted with ethyl acetate (3 x 20 mL). The organic phase was dried with anhydrous Na_2SO_4 and concentrated under reduced pressure. The product **6c** was purified by chromatography column using hexane: ethyl acetate (65:35) and obtained as a white solid (161 mg, 86 %); mp 98-100 ºC (lit.(Negrón-Silva et al., 2013) 102-104 °C); ^{1}H NMR (300 MHz, $CDCl_3$) δ 2.19 (t, *J* 2.4 Hz, 1H), 2.52 (t, *J* 2.4 Hz, 1H), 4.61 (d, *J* 2.4 Hz, 2H), 4.72 (d, *J* 2.4 Hz, 2H), 5.85 (d, *J* 7.8 Hz, 1H), 7.47 (d, *J* 7.8 Hz 1H); ^{13}C NMR (75 MHz, acetone-d_6) δ 30.51, 38.38, 71.75, 75.53, 78.19, 79.45, 101.95, 143.33, 151.00, 162.09; HRMS (ESI+) *m/z* calcd. for $C_{10}H_9N_2O_2$ $[M+H]^+$: 189.0658, found: 189.0668.

2.6. Synthesis of 3,7-dimethyl-1-propargylxanthine (6d)

In a 100 mL round-bottomed flask, equipped with a magnetic stirrer, were added a suspension of potassium carbonate (29.70 mmol, 4.10 g) in anhydrous DMF (30 mL), and theobromine (14.85 mmol, 2.67g). The mixture was stirred for one hour at room temperature followed by the addition of propargyl bromide (80 wt.% in toluene, 1.58 mL, 17.82 mmol). The reaction mixture was heated at 40 °C and stirred for 48 hours. After the reaction completion, the mixture was treated with brine (30 mL) and extracted with ethyl acetate (4 x 20 mL). The organic phase was dried with anhydrous Na_2SO_4 and concentrated under reduced pressure. The product **6d** was purified by recrystallization from hexane:ethyl acetate (1:1 v/v), and obtained as a 7hite solid (1.61 g, 50%); mp 204-205 ºC (lit.(Casaschi, Grigg & Sansano, 2000) 209 °C); ^{1}H NMR (300 MHz, DMSO-d_6) δ 3.09 (t, *J* 2.4 Hz, 1H), 3.42 (s, 3H), 3.88 (s, 3H), 4.58 (d, *J* 2.4 Hz, 2H), 8.05 (s, 1H); ^{13}C NMR (75 MHz, DMSO-d_6) δ 29.93, 30.36, 33.70, 73.26, 80.03, 106.89, 143.77, 148.89, 150.64, 153.88; HRMS (ESI+) *m/z* calcd. For $C_{10}H_{10}N_4O_2Na$ $[M+Na]^+$: 241.0695, found: 241.0690.

2.7. General procedure for the preparation of 1-(coumaronyl-triazolyl)uracil 7a,b 1-(coumaronyl-triazolyl)thymine 8a,b and 1-(coumaronyl-triazolyl)theobromine 10a,b

To a stirred solution of **6a**, **6b**, or **6d** (1 mmol) and 4-(azidomethyl)-coumarins **4a** or **4b** (1 mmol, 0.233 g for **4a** or 0.251 g for **4b**) **4a-b** (1 mmol) in ethanol water (10:1, 10 mL) was added

copper sulfate (0.027 mmol, 0.0068 g) and sodium ascorbate (0.072 mmol, 0.0125 g). The reaction mixture was kept under stirring at 30 °C, for 24 hours. After reaction completion, as indicated by TLC, the mixture was poured into an ice-water and the precipitate that formed was filtered and dried under vacuum.

2.7.1.1-((1-((5,7-dihydroxy-2-oxo-2H-chromen-4-yl)methyl)-1H-1,2,3-triazol-4-yl)methyl)pyrimidine-2,4(1H,3H)-dione (**7a**): white solid (306 mg, 80%); mp 230 ºC with degradation; ^{1}H NMR (300 MHz, DMSO-d_6) δ 4.64 (s, 1H), 4.99 (s, 2H), 5.59 (d, *J* 7.7 Hz, 1H), 5.99 (s, 1H), 6.03 (s, 2H), 6.16 (s, 1H), 7.77 (d, *J* 7.7 Hz, 1H), 8.21 (s, 1H), 11.33 (s, 1H, NH); ^{13}C NMR (75 MHz, DMSO-d_6) δ 42.55, 52.26, 62.84, 92.89, 99.76, 100.45, 101.31, 103.13, 125.01, 142.75, 145.70, 150.84, 153.74, 156.74, 160.48, 162.89, 163.83; HRMS (ESI+) *m/z* calcd. for $C_{17}H_{14}N_5O_6$ $[M+H]^+$: 384.0938, found: 384.0937.

2.7.2. 1-((1-((2-oxo-2H-benzo[h]chromen-4-yl)methyl)-1H-1,2,3-triazol-4-yl)methyl)pyrimidine-2,4(1H,3H)-dione (**7b**): white solid (352 mg, 88%); mp 235 ºC with degradation; ^{1}H NMR (300 MHz, DMSO-d_6) δ 4.98 (s, 2H), 5.58 (d, *J* 7.7 Hz, 1H), 5.93 (s, 1H), 6.06 (s, 2H), 7.70-7.79 (m, 3H), 7.82-7.91 (m, 2H), 8.04-8.07 (m, 1H), 8.29 (s, 1H), 8.35-8.40 (m, 1H), 11.34 (s, 1H, NH); ^{13}C NMR (75 MHz, DMSO-d_6) δ 42.55, 49.56, 101.28, 112.72, 113.20, 120.29, 121.65, 122.11, 124.25, 124.79, 127.62, 127.98, 129.07, 134.39, 143.12, 145.61, 150.07, 150.79, 150.90, 159.32, 163.74; HRMS (ESI+) *m/z* calcd. for $C_{21}H_{15}N_5O_4Na$ $[M+Na]^+$: 424.1016, found: 424.1001.

2.7.3. 1-((1-((5,7-dihydroxy-2-oxo-2H-chromen-4-yl)methyl)-1H-1,2,3-triazol-4-yl)methyl)-5-methylpyrimidine-2,4(1H,3H)-dione (**8a**): white solid (365 mg, 92%); mp 285 °C with degradation; ^{1}H NMR (300 MHz, DMSO-d_6) δ 1.75 (s, 3H), 4.80 (s, 1H), 4.95 (s, 2H), 5.94 (s, 2H), 6.22 (d, *J* 2.0 Hz, 1H), 6.30 (d, *J* 2.0 Hz, 1H), 7.65 (s, 1H), 8.18 (s, 1H), 11.32 (brs, 1H, NH); ^{13}C NMR (75 MHz, DMSO-d_6) δ 12.09, 42.46, 52.18, 94.94, 99.31, 100.06, 105.89, 109.06, 125.05, 141.40, 143.04, 150.88, 152.60, 156.46, 157.68, 160.05, 161.95, 164.50; HRMS (ESI+) *m/z* calcd. for $C_{18}H_{16}N_5O_6$ $[M+H]^+$: 398.1095, found: 398.1089.

2.7.4. 1-((1-((2-oxo-2H-benzo[h]chromen-4-yl)methyl)-1H-1,2,3-triazol-4-yl)methyl)-5-methylpyrimidine-2,4(1H,3H)-dione (**8b**): white solid (373 mg, 90%); mp 270-272 ºC; ^{1}H NMR

(300 MHz, DMSO-d_6) δ 1.74 (s, 3H), 4.94 (s, 2H), 5.94 (s, 1H), 6.06 (s, 2H), 7.64 (s, 1H), 7.72-7.74 (m, 2H), 7.81-7.91 (m, 2H), 8.03-8.06 (m, 1H), 8.28 (s, 1H), 8.35-8.38 (m, 1H), 11.33 (s, 1H, NH); ^{13}C NMR (75 MHz, DMSO-d_6) δ 12.00, 42.39, 49.59, 108.93, 112.71, 113.23, 120.27, 121.64, 122.10, 124.24, 124.83, 127.60, 127.96, 129.05, 134.38, 141.25, 143.32, 150.07, 150.78, 150.87, 159.33, 164.33; HRMS (ESI+) *m/z* calcd. for $C_{22}H_{18}N_5O_4$ $[M+H]^+$: 416.1353, found: 416.1358.

2.7.5. 1-((1-((5,7-dihydroxy-2-oxo-2H-chromen-4-yl)methyl)-1H-1,2,3-triazol-4-yl)methyl)-3,7-dimethyl-3,7-dihydro-1H-purine-2,6-dione (**10a**): white solid (410 mg, 91%); mp 315 ºC with degradation; ^{1}H NMR (300 MHz, DMSO-d6) δ 3.41 (s, 3H), 3.88 (s, 3H), 4.77 (s, 1H), 5.15 (s, 2H), 5.89 (s, 2H), 6.21 (d, J 2.4 Hz, 1H), 6.29 (d, J 2.4 Hz, 1H), 8.03 (s, 1H), 8.09 (s, 1H), 10.50 (s, 1H, OH), 11.05 (s, 1H, OH); ^{13}C NMR (75 MHz, DMSO-d6) δ 29.46, 33.19, 33.24, 35.98, 51.96, 94.80, 99.14, 99.89, 105.67, 106.65, 124.82, 143.14, 148.42, 150.73, 152.57, 154.05, 156.31, 157.51, 159.91, 161.81; HRMS (ESI+) m/z calcd. for $C_{20}H_{18}N_7O_6$ [M+H]+: 452.1313, found: 452.1326.

2.7.6. 3,7-dimethyl-1-((1-((2-oxo-2H-benzo[h]chromen-4-yl)methyl)-1H-1,2,3-triazol-4-yl)methyl)-3,7-dihydro-1H-purine-2,6-dione (**10b**): pale yellow solid (384 mg, 82%); mp 288–290 ºC; ^{1}H NMR (300 MHz, DMSO-d6) δ 3.41 (s, 3H), 3.87 (s, 3H), 5.14 (s, 2H), 5.93 (s, 1H), 6.03 (s, 2H), 7.70-7.78 (m, 2H), 7.84-7.92 (m, 2H), 8.04–8.08 (m, 2H), 8.19 (s, 1H), 8.36–8.40 (m, 1H); ^{13}C NMR (75 MHz, DMSO-d6) δ 29.45, 33.17, 35.94, 49.46, 106.64, 112.80, 113.30, 120.37, 121.66, 122.14, 124.25, 124.57, 127.65, 128.00, 129.08, 134.41, 143.11, 143.86, 148.43, 150.10, 150.72, 151.01, 154.06, 159.37; HRMS (ESI+) m/z calcd. for $C_{24}H_{20}N_7O_4$ [M+H]+: 470.1571, found: 470.1580.

2.8. General procedure for the preparation of 1,3-bis-(coumaronyl-triazolyl)uracil 9a and 9b.

To a stirred solution of 1,3-di(prop-2-yn-1-yl)pyrimidine-2,4(1*H*,3*H*)-dione **6c** (1 mmol, 0.188 g) and 4-(azidomethyl)-coumarin **4a** or **4b** (2 mmol, 0.466 g for **4a**; 0.502 g for **4b**) in ethanol water (10:1, 10 mL) was added $CuSO_4.7H_2O$ (0.055 mmol, 0.0136 g) and sodium ascorbate (0.143 mmol, 0.025 g). The reaction mixture was kept under stirring at 30 °C for 24 hours. After reaction

completion, as indicated by TLC, the mixture was poured into an ice-water and the precipitate that formed was filtered and dried under vacuum.

2.8.1 1,3-bis((1-((5,7-dihydroxy-2-oxo-2H-chromen-4-yl)methyl)-1H-1,2,3-triazol-4-yl)methyl)pyrimidine-2,4(1H,3H)-dione (**9a**): pale yellow solid (588 mg, 90%); mp 302 ºC with degradation; ^{1}H NMR (300 MHz, DMSO-d_6) δ 4.71 (s, 1H), 4.77 (s, 1H), 5.07 (s, 4H), 5.80 (d, *J* 7.7 Hz, 1H), 5.90 (s, 2H), 5.94 (s, 2H), 6.20 (d, *J* 2.4 Hz, 2H), 6.37 (d, *J* 2.4 Hz, 2H), 7.89 (d, *J* 7.7 Hz, 1H), 8.07 (s, 1H), 8.22 (s, 1H); ^{13}C NMR (75 MHz, DMSO-d_6) δ 36.02, 43.82, 52.15, 52.27, 62.93, 94.75, 99.55, 100.09, 100.69, 100.74, 105.29, 105.49, 124.99, 125.03, 125.32, 125.34, 142.58, 143.10, 144.61, 150.96, 152.77, 153.01, 156.42, 156.43, 158.19, 160.21, 160.23, 162.16, 162.18, 162.29; HRMS (ESI+) *m/z* calcd. for $C_{30}H_{23}N_8O_{10}$ $[M+H]^+$: 655.1531, found: 655.1527.

2.8.2. 1,3-bis((1-((2-oxo-2H-benzo[h]chromen-4-yl)me30thyl)-1H-1,2,3-triazol-4-yl)methyl)pyrimidine-2,4(1H,3H)-dione (**9b**): pale yellow solid (586 mg, 85%); mp 193-195 ºC; ^{1}H NMR (300 MHz, DMSO-d_6) δ 5.06-5.07 (m, 4H), 5.79 (d, *J* 7.7 Hz, 1H), 5.84 (s, 1H), 5.90 (s, 1H), 6.01 (s, 2H), 6.05 (s, 2H), 7.65-7.73 (m, 4H), 7.79-7.91 (m, 5H), 7.99-8.02 (m, 2H), 8.16 (s, 1H), 8.27-8.30 (m, 3H); ^{13}C NMR (75 MHz, DMSO-d_6) δ 35.86, 43.81, 49.52, 49.62, 100.63, 112.69, 113.00, 113.06, 120.24, 121.60, 122.07, 124.29, 124.73, 125.03, 127.59, 127.95, 129.04, 134.38, 142.89, 143.32, 144.49, 150.02, 150.84, 150.93, 151.10, 159.37, 162.12; HRMS (ESI+) *m/z* calcd. for $C_{38}H_{27}N_8O_6$ $[M+H]^+$: 691.2048, found: 691.2034.

2.9. General procedure for the preparation of inclusion complex and dilution

1 mL of an ethanolic solution containing the compound **7a**,**b**, **8a,b**, **9a,b** or **10a**,**b** (0.004 mol L^{-1}) was vigorously stirred with 1 mL of an aqueous solution of HP-β-CD (0.004 mol L^{-1}). The resulting mixture was kept under stirring until a clear solution is obtained. The final solution was concentrated under vacuum to remove the solvent, and the remaining water was removed by lyophilization to give a water-soluble compound-HP-β-CD complex in a powder form (Melo et al., 2007). The stock solutions of the compounds were prepared by dissolving the complexed compounds in 200 µL of DMSO, followed by dissolving in 1800 µL of Dulbecco's Modified Eagle Medium (DMEM). The stock solution and dilutions were prepared prior of the cytotoxicity assays.

2.10. Cells cultures

The human colon carcinoma (HCT116), human laryngeal tumor cells (Hep-2), and human lung carcinoma cells (A549) cell lines, and the non-tumor human keratinocyte cell line (HaCat) were purchased from Rio de Janeiro Cell Bank. The cells were maintained in DMEM supplemented with 10% fetal bovine serum (FBS, Gibco BRL; Life Technologies) and 1% penicillin-streptomycin in a humidified 5% CO_2 atmosphere, at 37 °C.

2.11. Cell viability MTT Assay

The cytotoxicity was assayed through the colorimetric microculture MTT assay. Cell suspensions were plated in 96-well plates in triplicate at an initial density of 07 x 10^4 cells mL^{-1} and incubated at 37 ºC for 24 h. After the incubation, the cells were treated with various concentrations of the evaluated compounds (**7a**,**b**, **8a,b**, **9a,b** or **10a**,**b**) and incubated for 24 and 48 h. After the treatment, the medium was removed, and an MTT solution (0.4 mg mL^{-1}) was added to each well and further incubated for 2 h at 37 ºC. Then, DMSO (100 µL) was added for solubilization of the formazan crystals and the absorbance intensities were measured in a microplate reader (SpectraMax M2e, Molecular devices, USA) at 570 nm. The percentage of viable cells was calculated in relation to the control to determine the cytotoxic concentration that reduces 50% of the cell viability (IC_{50}).

2.12. Biological Target and Toxicity Prediction

The shared scaffold of uracil, coumarin and triazole, such as (1-((1-((5,7-dihydroxy-2-oxo-2*H*-chromen-4-yl)methyl)-1*H*-1,2,3-triazol-4-yl)methyl)-3-methylpyrimidine-2,4(1*H*,3*H*)-dione), from the structures of compounds **9a**,**b** and **10a**,**b** were submitted to the evaluation of potential risk to cause mutagenic, tumorigenic, irritant effects and on the reproductive system, with the employment of Osiris Property Explorer® software (Sander et al., 2009) available free from web (https://www.organic-chemistry.org/prog/peo/). Similarity Ensemble Approach (SEA) virtual target screening server (Keiser et al., 2007) was used to predict the potential binding biological targets. Chemical structures of more active compounds and also the main fragments of them were described in smiles sequences before performing the software.

2.13. Molecular modeling and docking studies

All molecular modeling studies were performed with more active compounds 9a,b and 10a,b, aiming to find information that may support the understanding of the biological activity. Geometry optimization and conformational analysis were calculated using Spartan'08® modelling software (V. 1.2.0, Wavefunction Inc., Irvine, USA)(Spartan '08, Version 1.2.0; Wavefunction, Inc.; Irvine, CA 92612, USA) based on the DFT-B3LYP/6-311G* method, set in gas phase. The geometry of compounds was optimized followed by submitting to systematic conformational analysis with torsion angle increment set of 30° in the range 0-360°. The lowest energy conformer for the chemical structure was saving in mol2 file before to use in docking studies. The structure of human DNA topoisomerase 1 (Topo-1) encoded by PDB ID: 1K4S (Staker et al., 2002) was downloaded from Protein Data Bank (PDB, http://www.rcsb.org/pdb), before to perform the docking studies. The cavity of interaction from Topo-1 model was used in this study. The protein structure was prepared by removing the water molecules and adding polar hydrogens using Autodock Tools (version 1.5.6) (Morris et al., 2009)**.** Docking studies were performed using iGemdock software (version 2.1) (Yang & Chen, 2004) in which the individual binding poses of compounds were assessed and submitted to dock in the protein. Docking calculations were performed at drug screening Docking Accuracy Setting with generic evolutionary method (GA) parameters set for population size, generation, and the number of solutions as 200, 70, and 8, respectively, ligand entry energy option active, and Gemdock score function of hydrophobic and electrostatic (1:1 preference). iGemdock software was used to propose the pharmacological pose interactions between the biological receptor and the compound studied.

3. Results and Discussion

3.1. Chemistry

The synthetic protocol to obtain the target hybrid compounds started with the Pechmann condensation of the phenols phloroglucinol (**1a**) and 1-naphthol (**1b**) with the β-ketoester ethyl 4-chloroacetoacetate (**2**) to achieve the 4-chloromethylcoumarins **3a** and **3b** with 86 and 70% yield, respectively. This procedure was carried out in the absence of solvent and using sulfamic acid as catalyst (Moraes, Lenardão & Barcellos, 2021). Then, the azide group was installed by the nucleophilic displacement of the chlorine atom (Naik et al., 2012), affording the 4-(azidomethyl)coumarins **4a** and **4b** with 89 and 86% yields, respectively, as shown in Figure 2.

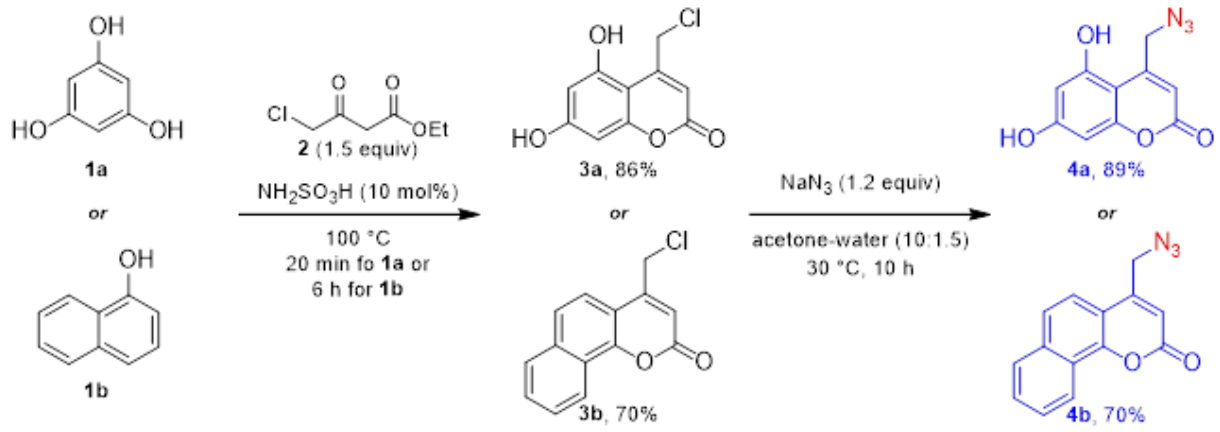

Figure 2. Synthesis of the 4-(azidomethyl)coumarins **4a** and **4b.**

Next, we prepare the portions constituted by the *N1*-propargylated uracil (**6a**) *N1*-propargylated thymine (**6b**), or *N1,N2*-dipropargylated uracil (**6c**). Initially, we envisioned the monopropargylation reaction of the nucleobases at the *N*1-position, retaining the hydrogen at the *N3*-position free, due to its importance in biological activity. The preservation of the hydrogen at the *N3*-position is intended to maintain the same hydrogen-bond pairing scheme presented by uracil. In addition, the propargylation at *N1*-position is necessary to introduce lipophilic groups or to bind other groups to the nucleobase skeleton (Accetta et al., 2009).

Thus, to prepare selectively the *N1*-propargylated nucleobases **6a**,**b**, the bis(trimethylsilyl)acetamide (BSA) was employed as base, using acetonitrile as solvent, at 45 °C for 72 hours (González-Olvera et al., 2013). This methodology allows us to obtain the desired compounds as unique products with 62% and 76% yield for **6a** and **6b**, respectively (Fig. 3). Afterward, the *N1,N2*-dipropargylated uracil **6c** was synthesized in order to obtain the hybrid compounds bis-(coumaronyl-triazolyl)uracil, which is based on similar molecular structures that present anticancer activity (Kumar et al., 2012). In this case, the dipropargylation reaction was carried out using the simple base K_2CO_3 in anhydrous DMF, at room temperature, for 24 hours. The *N1,N2*-dipropargylated uracil **6c** was obtained with 86% (Fig. 3, Scheme A).

In addition to the uracil and thymine, we also decided to investigate the influence of the theobromine (**5c**, 3,7-dimethylxanthine) moiety in the activity. The propargylated theobromine (**6d**) was prepared using K_2CO_3 as base, in anhydrous DMF, at 40 °C (Kumar et al., 2012). However, a longer reaction time of 48 h was necessary to achieve only 50% yield (Figure 3, Scheme B).

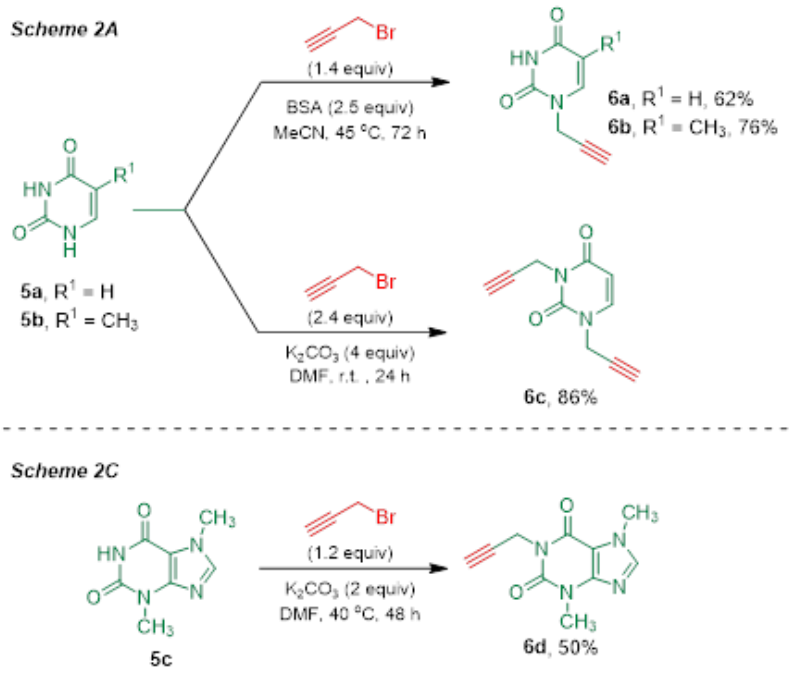

Figure 3. Synthetic methodologies employed to prepare the *N1*-propargylated uracil **6a**, the *N1*-propargylated thymine **6b**, the *N1*,*N2*-dipropargylated uracil **6c**, and the propargylated theobromine **6d**.

Theobromine is an alkaloid of the family of methylxanthines. It is found mainly in cocoa products and has a diuretic action (Barreto Alves & Bragagnolo, 2002). Besides, theobromine derivatives demonstrated potential antitumor activities through multiple mechanisms and could reverse resistance to multiple drugs. In view of this potential, theobromine derivatives can lead to potent antitumor agents, selective and with low toxicity (Johnson et al., 2012; Ma et al., 2019).

The propargylated nucleobases **6a-d** and the 4-(azidomethyl)coumarins **4a**,**b** were hybridized through a 1,2,3-triazole ring by a Cu(I)-catalyzed [3+2]-cycloaddition reaction, as outlined in Fig 4. The click reaction was successfully employed for all intermediates, using the simple copper(II) sulfate and sodium ascorbate system to generate the copper(I) catalyst. All the reactions were carried out in ethanol-water (10:1), at 30 °C, for 24 hours.

After the reaction completion, the target compounds were simply purified by pouring the reaction contents into an ice-water mixture. The precipitated products were filtered and present a high purity degree, as observed by ^{1}H NMR. However, when impurities were noticed, they were removed by a short pad of silica gel. The target compounds **7a,b**, **8a,b**, **9a,b**, and **10a,b** were prepared from good to excellent yield as shown in Figure 4.

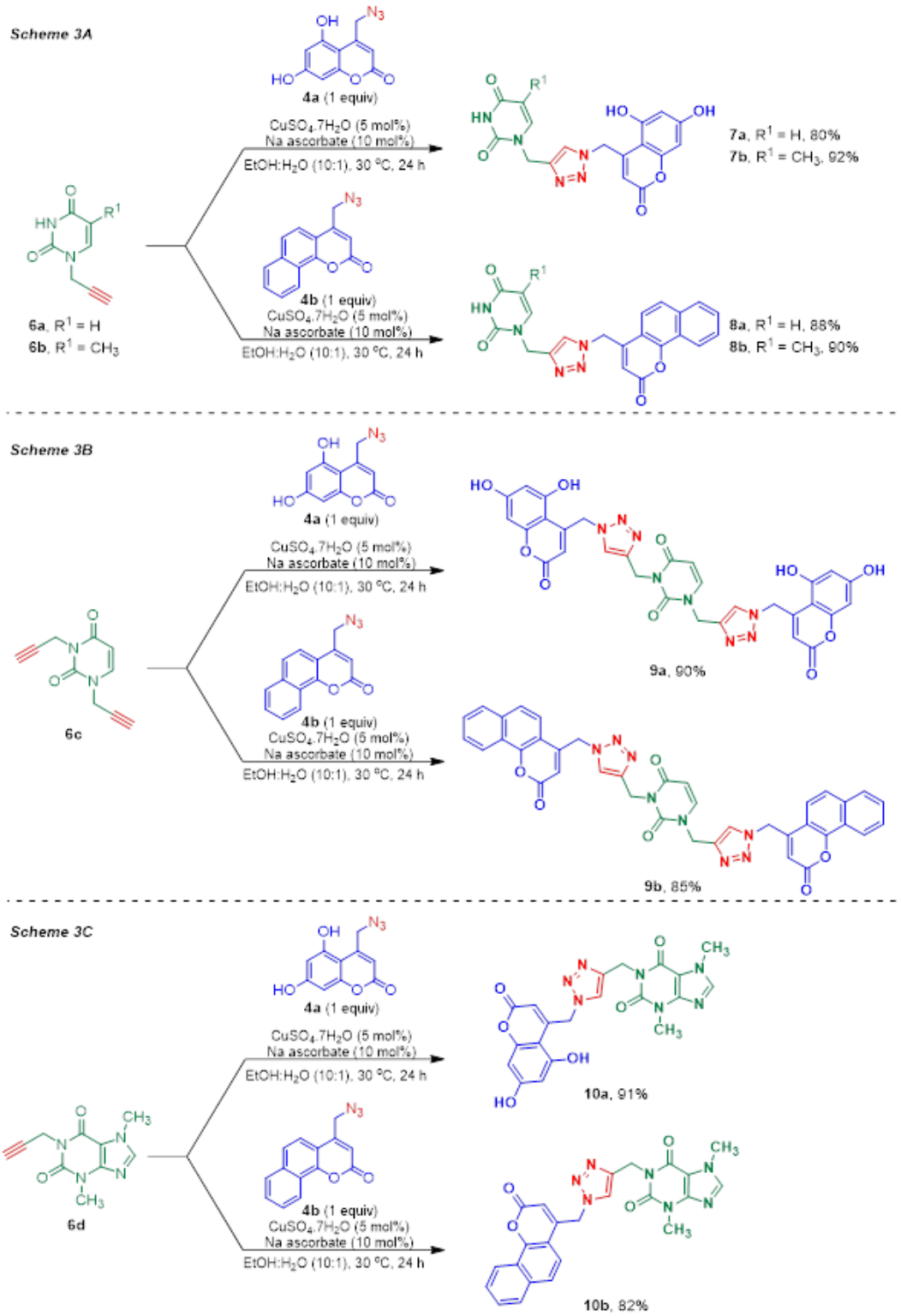

Figure 4. Cu(I)-catalyzed [3+2]-cycloaddition reaction between the 4-(azidomethyl)coumarins **4a**,**b**, and the *N*1-propargylated uracil **6a**, *N*1-propargylated thymine **6b** (Scheme 3A), *N1*,*N2*-dipropargylated uracil **6c** (Scheme 3B) and the propargylated theobromine **6d** (Scheme 3C), leading to the corresponding target hybrid molecules.

All compounds were characterized by ^{1}H and ^{13}C NMR, HRMS, and melting point. The NMR spectra for the final compounds are reported in the Supplementary Information.

3.2. Inclusion complex

Before the cytotoxic evaluation, it was noticed that the target compounds show low solubility in the cell medium, even the *N1*-(cumaronyltriazolyl)uracils **7a,b** and **8a,b**, with the free hydrogen at *N3*-position. In order to enhance the solubility, we proposed the use of non-toxic (2-hydroxylpropyl)-β-cyclodextrin (HP-β-CD) as a complexing agent. The HP-β-CD is suitable for cell culture and has been used to enhance the solubility of non-polar compounds, such as vitamins and hormone derivatives (Saokham et al., 2018). Hydrophobic molecules are incorporated into the cavity by water molecules displacement, thus favoring the solubility in the medium. During the cytotoxic experiment, the reverse process occurs due to low concentration, releasing the active compound. Thus, the complex compounds were prepared by vigorous mixing of a solution of the targets in ethanol, with an equimolar amount of HP-β-CD in water. After 15 h of vigorous mixing, it is noticed a clean solution, which in turn the solvent was removed under vacuum, and the residual water was removed by lyophilization to obtain a solid. The complex compounds were characterized by ^{1}H NMR and, besides the presence of HP-β-CD signals, no significant changes in the chemical shift of the signals of the target compounds were noticed.

3.3. Biological activities

3.3.1. Cytotoxicity assay

The potential antitumor activity of eight new hybrids was evaluated through colorimetric microculture MTT assay against three tumor cell lines: human colon carcinoma cells (HCT116), human laryngeal tumor cells (Hep-2), and human lung carcinoma cells (A549). The hybridized compounds were also assayed against the non-tumor cell line HaCat (human keratinocyte) in order to obtain an indication of their selective cytotoxicity. Also, the commercial anticancer drug doxorubicin was employed as a positive drug standard to compare the cytotoxicity activities. Each experiment was carried out in triplicate on three different days. The selectivity index (SI) was calculated as the ratio between the IC_{50} (concentration that reduces cell viability by 50%) of HaCat (non-tumor line) and the IC_{50} of tumor lines. The results are outlined in Table 1.

The mono *N1*-(coumaronyltriazolyl)uracils **7a,b** and **8a,b** did not show activity against the tumor cell lines, with the exception of the compound **8b**, which showed poor cytotoxicity only against HCT116 cells with an IC_{50} of 87.58 ± 1.94 μM. The compound **9a**, resulting from the molecular hybridization of the uracil and two coumarins derived from phloroglucinol, exhibits the highest cytotoxicity against HCT116 cells with an IC_{50} of 24.19 ± 1.39 μM for a 48 h experiment (Table 1, entry 1). Interestingly, the compound **9a** did not exhibit appreciable cytotoxicity against the non-tumor cells HaCat showing a good selectivity index (SI) of 6.0. No cytotoxicity effect was observed for compound **9a** against A549 cells in 24 and 48 h treatment. For Hep-2 cells, an IC_{50} of 51.55 ± 1.71 μM was noticed for 24 h of exposure.

The compound **9b**, which is analog to **9a**, but with the coumarin moiety derived from 1-naphthol, presented an IC_{50} for HCT116 cells of 54.50 ± 1.74 and 59.17 ± 1.77 μM for 24 and 48 h treatment. It was the only compound in the series that showed activity against A549 cells, with an IC_{50} of 51.03 ± 1.71 μM for 24 h of exposure. Besides the moderated cytotoxicity, the selectivity index when compared to HaCat cells was 63. No appreciative cytotoxicity was observed for Hep-2 cells.

The compounds **10a**,**b**, both derived from the nucleobase theobromine, showed activity against HCT116 cells. However, the compound **10b** showed higher potency with an IC_{50} 40.98 ± 1.61 μM for 24 h of exposure with a selectivity index of 6. Compounds with SI ≥ 10 can be considered selective (Peña-Morán et al., 2016). The compound **10a** showed an IC_{50} of 78.26 ± 1.89 in 24 h of exposure for HCT116 cells, and an IC_{50} of 56.55 ± 1.75 μM for Hep-2 cells, with a selectivity index of 4 and 5, respectively. None of the tested compounds showed cytotoxicity against the non-tumor cell line (HaCat), even at the highest evaluated concentration of 100 μM at all exposure times tested. Also, the reference compound doxorubicin was used as a positive drug standard to compare the cytotoxicity activities. For the HCT116 cell line, the compound **9a** showed a moderated activity (approximately 20-fold) when compared to doxorubicin (IC_{50} of 1.23 ± 0.05 μM).

Table 1. Compounds assessed in this study and their cytotoxicity against three different cell lines by the colorimetric MTT assay.

Compound	IC_{50} (µM ± SD)[a]							
	HCT116		A549		Hep-2		HaCat	
	24 h	48 h	24 h	48 h	24 h	48 h	24 h	48 h
7a	>100	>100	>100	>100	>100	>100	>100	>100
7b	>100	>100	>100	>100	>100	>100	>100	>100
8a	>100	>100	>100	>100	>100	>100	>100	>100
8b	87.58 ± 1.94	>100	>100	>100	>100	>100	454.1 ± 2.67	>100
9a	69.22 ± 1.85	24.19 ± 1.39	>100	>100	51.55 ± 1.71	>100	634.9 ± 2.80	141.6 ± 2.15
9b	54.50 ± 1.74	59.17 ± 1.77	>100	51.03 ± 1.71	>100	>100	1049 ± 3.02	3228 ± 3.5
10a	78.26 ± 1.89	>100	>100	>100	56.55 ± 1.75	>100	307.8 ± 2.49	>100
10b	40.98 ± 1.61	84.74 ± 1.92	>100	>100	>100	>100	263.3 ± 2.42	119.6 ± 2.08
Doxorubicin[b]	-	1.23 ± 0.05	n.d	n.d	-	1.69 ± 0.15	-	39.32 ± 1.59

[a]SD, Standard deviation (n = 3). [b]Doxorubicin was used as positive controls against HCT116, HEP-2 and HaCat cell lines. HCT116: human colon carcinoma cells; A549: human lung carcinoma cells; Hep-2: human laryngeal tumor cells; HaCat: human keratinocyte. N.d.: IC_{50} for the positive control was not measured for A459 cell line due to a lack of activity of the target compounds.

3.4. In silico studies

The Osiris Property Explorer (Sander et al., 2009) software was used to calculate the mutagenic, tumorigenic, irritant, and toxicant reproductive system effects of the compounds **9a**,**b** and **10a,b**, and therefore, to predict the toxicity risks. The calculations are based on the functional group similarity between the query molecule within the compounds present in the software database. The results were compared with the standard H_2O_2 and are outlined in Table 2.

The evaluation showed that compounds **9a** and **9b** showed a low risk of causing theoretical mutagenic and also the tumorigenic effect. No risk of irritant effect was determined. Only compound **9a** showed the medium risk to cause an effect on the reproductive system. All compounds showed lower predicted toxic effects in comparison with H_2O_2. These results suggest the compounds present low potential to cause theoretical toxicity risks, and these are able to be submitted to drug design development.

Table 2. Prediction of theoretical toxicity of **9a,b**, **10a,b** in comparison with H_2O_2.[a]

Toxicity risk	9a	9b	10a	10b	H_2O_2
Mutagenic	–	+	–	+	+++
Tumorogenic	–	+	–	+	+++
Irritant	–	–	–	–	+++
Reproductive system	++	–	–	–	+

[a]The scale of risk of toxicity varies from none (–), low (+), medium (++), and high (+++) calculated using the Osiris Property Explorer® software.[39]

In order to understand the cytotoxicity presented by the compounds in the MTT assay, we decided to employ computational techniques to suggest the most likely biological target. The chemical similarity ensemble algorithm (SEA) (Keiser et al., 2007) was employed based on the hypothesis of the identification of candidate target proteins to interact with the shared scaffolds of uracil, coumarin and triazole, such as (1-((1-((5,7-dihydroxy-2-oxo-2H-chromen-4-yl)methyl)-1H-1,2,3-triazol-4-yl)methyl)-3-methylpyrimidine-2,4(1H,3H)-dione), from the structures of **9a**, **9b**, **10a**, and **10b**. The results indicated potential several proteins targets, in which the main target model is related to DNA topoisomerase 1 (Topo-1), which showed a p-value of 3.83 e^{-31} and maximum Tanimoto coefficient (max-TC) of 0.29. All predicted results are shown in Table 3.

Table 3. Main biological target candidates identified by SEA predictions.

Description	p-value	maxTC
DNA topoisomerase 1	$3.83e^{-31}$	0.29
Low molecular weight phosphotyrosine phosphatase	$6.667e^{-30}$	0.30
Testosterone 17-β-dehydrogenase 3	$1.506e^{-20}$	0.37

maxTC: maximum Tanimoto coefficient

Topoisomerase inhibitors have been shown to be potent antineoplastic agents. The explanation for this potential is due to the mechanism of action of topoisomerase-targeted drugs; the higher the cellular concentration of topoisomerases, the more lethal these drugs become. Tumor cells grow faster and generally express higher concentrations of topoisomerase than normal cells. Therefore, drugs generate more DNA breaks and are more toxic to tumor cells (Deweese, Osheroff & Osheroff, 2009).

Compounds containing triazole, coumarin, or uracil nucleus in their structures have shown antitumor activity attributed to topoisomerase inhibitory activity (Guruge, Udawatte & Weerasinghe, 2016; Xu et al., 2016; Li et al., 2017), which could indicate the importance of these cores in the construction of new molecules aimed at this biological target. Thus, according to the obtained results, the DNA topoisomerase 1 was selected as the target protein in further docking studies.

3.5. Molecular modeling and docking studies

For the docking analyses, the lowest-energy molecular conformers for the most active compounds **9a,b** and **10a,b** were generated by Spartan'08 modelling software (Spartan '08, Version 1.2.0; Wavefunction, Inc.; Irvine, CA 92612, USA). Further, the docking studies were performed to identify the individual pose that presents lower energy that selectively binds to the DNA topoisomerase-1 active site. The molecular docking analysis was accomplished by using the iGEMDOCK software (version 2.1) (Yang & Chen, 2004)**.** applying the generic evolutionary method (GA). The empirical scoring function was measured using the total sum of the energies of van der Waal forces (VDW), hydrogen bond (H-bond), and electrostatic interactions occurring between the compounds and the target protein, as shown in Table 4.

The compound **9a** was the ligand with the lowest energy in the series, with a total binding energy of –118.5 kcal mol^{-1}. The ligands **9b** and **10a** show similar total binding energy values, which are –113.3 and –113.7 kcal mol^{-1}, respectively. However, for ligand **9b** the contribution of van der Waal energy was larger than to ligand **10a**. In turn, the contribution of H-bond energy for ligand **10a** was larger than to ligand **9b**. The ligand **10b** showed the lowed the highest total binding energy in the series, with a value of –102.7 kcal mol^{-1}.

Table 4. Calculated total energy (kcal mol^{-1}) of compounds **9a,b** and **10a,b** derivatives on the DNA topoisomerase 1.[a]

Compound	Total binding energy[b]	VDW	H-bond	Electrostatic interactions
9a	–118.5	–85.6	–32.9	0
9b	–113.3	–91.5	–21.8	0
10a	–113.7	–68.4	–45.3	0
10b	–102.7	–80.9	–21.8	0

[a]All energy values are given in kcal mol^{-1}. [b]Total binding energy = VDW + H-Bond + electrostatic interactions. VDW: van der Waal forces; H-bond: hydrogen bond.

Considering the interaction with the amino acid residues in the active site of Topo-1, the docking studies reveal that the main interactions occur with the residues: ARG 364, ARG 488 LYS 532, ASP 533, ILE 535, HIS 632, THR 718, LEU 721, ASN 722, TYR 723 (O-phospho-L-tyrosine), and LYS 571, as illustrated in Fig. 5A. The measured energies are represented in Table 5. The residues ARG 364, LYS 532, ASP 533, ASN 722, and TYR 723 are the same observed in docking studies performed by Laco (2011) (Laco, 2011), who suggest the same active site of Topo-1 herein studied.

In the post-screening analysis using Residues Consensus Analysis, HIS 632 was detected as the main residue evolved in this ligand-receptor binding (with Z-score 1.94 and WPharma 1.00).

Van der Waals interactions are the main type between the ligands and the residues in the binding site of Topo-1. Some relevant interactions to compounds poses are observed to LYS 532, HIS 632, and LEU 721. The main molecular regions of interaction between **9a** and Topo-1 in the *in silico* model are shown in Figure 5B. The carbonyl group from the coumarin moiety showed relevant interaction with HIS 632, while the uracyl moiety interacts with ARG 364 and THR 718. One of the triazole rings showed interaction with ARG 364 from Topo-1. Thus, based on the results from the docking studies, the most active compound, are potential ligands and fits as candidates as Topo-1 inhibitors.

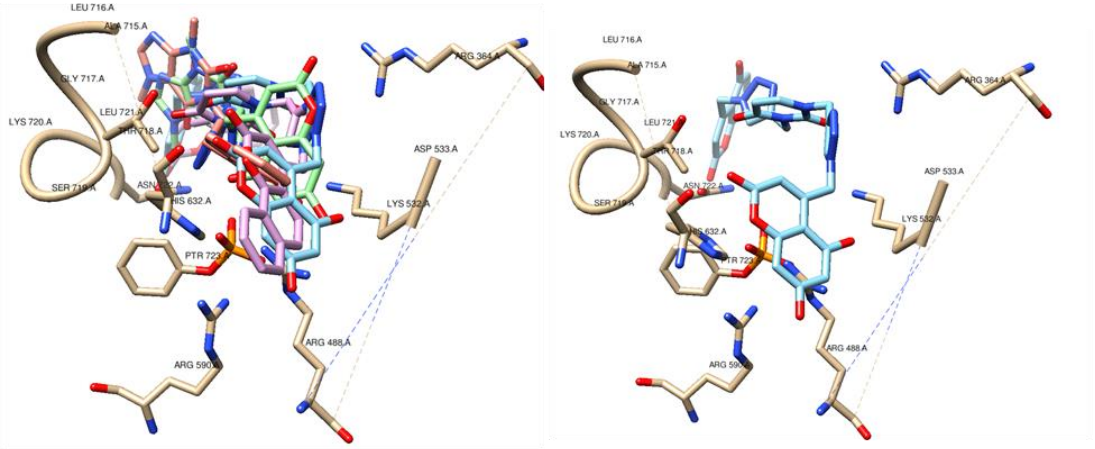

Figure 5. Predicted binding of the most active in vitro compounds 9a,b and 10a,b poses (A) and 9a pose (B) in the active site of Topo-1 (PDB code: 1K4S). Graphic visualization obtained using UCSF Chimera (v.1.10.1).[47]

Table 5. Van der Waals (VDW), and H-bonding (H-bond) pharmacological interactions between ligands **9a,b**, **10a,b**, and the amino acid residues in the binding site of Topo-1 applying the Residues Consensus Analysis.[a]

Amino acid residues	Ligand							
	9a		9b		10a		10b	
	VDW	H-bond	VDW	H-bond	VDW	H-bond	VDW	H-bond
ARG 364	–5.8	0.0	–4.1	0.0	–1.5	0.0	0.0	0.0
ARG 488	–4.4	–3.4	–3.8	0.0	1.5	–6.3	–4.5	–7.0
LYS 532	–10.2	–4.2	–8.7	0.0	–9.0	–2.2	–1.0	–3.5
ASP 533	1.6	–10.5	–4.7	–8.2	–5.7	–2.5	–0.8	0.0
ILE 535	–16.7	0.0	–15.0	0.0	–4.1	0.0	–1.6	0.0
HIS 632b	–13.6	–3.5	–21.1	0.0	–4.6	–3.5	–22.5	0.0
THR 718	–3.8	0.0	–5.7	0.0	–6.0	0.0	–5.6	0.0
LEU 721	–9.5	0.0	–2.7	0.0	–13.6	0.0	–19.3	0.0
ASN 722	–1.2	–3.5	–7.3	0.0	–4.4	–3.5	–6.3	–9.9
TYR 723	–0.4	0.0	–2.0	0.0	–4.0	–9.3	–7.3	–4.2
LYS 751	0.0	–7.0	0.0	–3.5	0.0	0.0	0.0	0.0

[a]All energy values are given in kcal mol^{-1}. [b]Confirmed by Residues Consensus Analysis. VDW: van der Waal forces; H-bond: hydrogen bond

4. Conclusion

In conclusion, we described the synthesis of eight novel compounds originated from the molecular hybridization of the nucleobases uracil, thymine, or theobromine, with coumarins linked through triazoles rings. Among the synthesized compounds, the hybrid compound **9a**, composed of uracil and the coumarin derivative phloroglucinol, showed antitumor activity against colon carcinoma (HCT116) with the lowest value of IC_{50} of 24.19 ± 1.39 μM and selectivity index of 6.0. The finding *in vitro* results were supported by *in silico* experiments that, according to SEA algorithm, the synthesized compounds show affinity to DNA Topoisomarase-1. Also, molecular docking studies demonstrate that the target compounds **9a**,**b** and **10a**,**b** are potential ligands for

Topo-1 protein and possibly acting as its inhibitor. Thus, these findings support the potential antitumor activity revealed by these compounds since Topo-1 has been identified as a potential biological target for several anticancer drugs. This protein complex is more expressed in tumor cells than in normal cells. Lastly, *in silico* toxicity prediction studies have shown that the target compounds possess low risk of causing theoretical mutagenic and tumorigenic effects compared to H_2O_2. Thus, based on the low cytotoxicity showed by the compounds **9a**,**b** and **10a**,**b**, they can be considered as lead scaffolds for further studies.

5. Acknowledgments

Authors are grateful to Conselho Nacional de Desenvolvimento Científico e Tecnológico – CNPq (N° 431084/2018-1) for financial support. Coordenação de Aperfeiçoamento de Pessoal de Nível Superior - Brasil (CAPES) - Finance Code 001, is also acknowledged for the doctoral fellowship of M.C.M., who also thanks IFRS (Federal Institute of Education, Science and Technology of Rio Grande do Sul) for the financial support.

6. Author Contributions

Maiara C. de Moraes – Conceptualization, Investigation, Writing original draft, Writing-review & editing; Rafaele Frassini – investigation; Mariana Roesch-Ely – Resources; Favero R. Paula –, Investigation, Software, Writing original draft; Thiago Barcellos – Conceptualization, funding acquisition, Resources, Writing original draft, Writing-review & editing.

7. Supplementary Information

Supplementary information for this article (Copies of ^{1}H and ^{13}C NMR of all new compounds) can be found online at.

8. References

Abbasi Z, Rezayati S, Bagheri M, Hajinasiri R. 2017. Preparation of a novel, efficient, and recyclable magnetic catalyst, γ-Fe2O3@HAp-Ag nanoparticles, and a solvent- and halogen-free protocol for the synthesis of coumarin derivatives. *Chinese Chemical Letters* 28:75–82. DOI: 10.1016/j.cclet.2016.06.022.

Accetta A, Corradini R, Sforza S, Tedeschi T, Brognara E, Borgatti M, Gambari R, Marchelli R. 2009. New uracil dimers showing erythroid differentiation inducing activities. *Journal of*

Medicinal Chemistry 52:87–94. DOI: 10.1021/jm800982q.

Akkol EK, Genç Y, Karpuz B, Sobarzo-Sánchez E, Capasso R. 2020. Coumarins and coumarin-related compounds in pharmacotherapy of cancer. *Cancers* 12:1–25. DOI: 10.3390/cancers12071959.

Barreto Alves A, Bragagnolo N. 2002. Simultaneous determination of theobromine, theophylline and caffeine in teas by high performance liquid chromatography. *Revista Brasileira de Ciencias Farmaceuticas/Brazilian Journal of Pharmaceutical Sciences* 38:237–243. DOI: 10.1590/s1516-93322002000200013.

Casaschi A, Grigg R, Sansano JM. 2000. Palladium catalysed tandem cyclisation-anion capture. Part 6: Synthesis of sugar, nucleoside, purine, benzodiazepinone and β-lactam analogues via capture of in situ generated vinylstannanes. *Tetrahedron* 56:7553–7560. DOI: 10.1016/S0040-4020(00)00661-X.

Claudio Viegas-Junior, Eliezer J. Barreiro, Carlos Alberto Manssour Fraga. 2007. Molecular Hybridization: A Useful Tool in the Design of New Drug Prototypes. *Current Medicinal Chemistry* 14:1829–1852. DOI: 10.2174/092986707781058805.

Dandriyal J, Singla R, Kumar M, Jaitak V. 2016. Recent developments of C-4 substituted coumarin derivatives as anticancer agents. *European Journal of Medicinal Chemistry* 119:141–168. DOI: 10.1016/j.ejmech.2016.03.087.

Deshmukh TR, Khare SP, Krishna VS, Sriram D, Sangshetti JN, Bhusnure O, Khedkar VM, Shingate BB. 2019. Design and Synthesis of New Aryloxy-linked Dimeric 1,2,3-Triazoles via Click Chemistry Approach: Biological Evaluation and Molecular Docking Study. *Journal of Heterocyclic Chemistry* 56:2144–2162. DOI: 10.1002/jhet.3608.

Deweese JE, Osheroff MA, Osheroff N. 2009. DNA topology and topoisomerases: Teaching A "knotty" subject. *Biochemistry and Molecular Biology Education* 37:2–10. DOI: 10.1002/bmb.20244.

Emami S, Dadashpour S. 2015. Current developments of coumarin-based anti-cancer agents in medicinal chemistry. *European Journal of Medicinal Chemistry* 102:611–630. DOI: 10.1016/j.ejmech.2015.08.033.

Gao F, Ye L, Kong F, Huang G, Xiao J. 2019. Design, synthesis and antibacterial activity evaluation of moxifloxacin-amide-1,2,3-triazole-isatin hybrids. *Bioorganic Chemistry* 91:103162. DOI: 10.1016/j.bioorg.2019.103162.

Gazivoda Kraljević T, Ilić N, Stepanić V, Sappe L, Petranović J, Kraljević Pavelić S, Raić-Malić S. 2014. Synthesis and in vitro antiproliferative evaluation of novel N-alkylated 6-isobutyl- and propyl pyrimidine derivatives. *Bioorganic and Medicinal Chemistry Letters* 24:2913–2917. DOI: 10.1016/j.bmcl.2014.04.079.

Gomha SM, Abdel-aziz HM, Abolibda TZ, Hassan SA, Abdalla MM. 2020. Green synthesis, molecular docking and pharmacological evaluation of new triazolo-thiadiazepinylcoumarine derivatives as sedative-hypnotic scaffold. *Journal of Heterocyclic Chemistry* 57:1034–1043. DOI: 10.1002/jhet.3827.

Gomha SM, Abdel-aziz HM, El-Reedy AAM. 2018. Facile Synthesis of Pyrazolo[3,4-c]pyrazoles Bearing Coumarine Ring as Anticancer Agents. *Journal of Heterocyclic Chemistry* 55:1960–1965. DOI: 10.1002/jhet.3235.

Gonçalves GA, Spillere AR, das Neves GM, Kagami LP, von Poser GL, Canto RFS, Eifler-Lima VL. 2020. Natural and synthetic coumarins as antileishmanial agents: A review. *European Journal of Medicinal Chemistry* 203. DOI: 10.1016/j.ejmech.2020.112514.

González-Olvera R, Espinoza-Vázquez A, Negrón-Silva GE, Palomar-Pardavé ME, Romero-Romo MA, Santillan R. 2013. Multicomponent click synthesis of new 1,2,3-triazole derivatives of pyrimidine nucleobases: Promising acidic corrosion inhibitors for steel. *Molecules* 18:15064–15079. DOI: 10.3390/molecules181215064.

Guruge AG, Udawatte C, Weerasinghe S. 2016. An in silico approach of coumarin-derived inhibitors for human DNA Topoisomerase i. *Australian Journal of Chemistry* 69:1005–1015. DOI: 10.1071/CH16232.

Ivasiv V, Albertini C, Gonçalves AE, Rossi M, Bolognesi ML. 2019. Molecular Hybridization as a Tool for Designing Multitarget Drug Candidates for Complex Diseases. *Current Topics in Medicinal Chemistry* 19:1694–1711. DOI: 10.2174/1568026619666190619115735.

Johnson IM, Prakash H, Prathiba J, Raghunathan R, Malathi R. 2012. Spectral Analysis of Naturally Occurring Methylxanthines (Theophylline, Theobromine and Caffeine) Binding with DNA. *PLoS ONE* 7. DOI: 10.1371/journal.pone.0050019.

Keiser MJ, Roth BL, Armbruster BN, Ernsberger P, Irwin JJ, Shoichet BK. 2007. Relating protein pharmacology by ligand chemistry. *Nature Biotechnology* 25:197–206. DOI: 10.1038/nbt1284.

Kerru N, Singh P, Koorbanally N, Raj R, Kumar V. 2017. Recent advances (2015–2016) in

anticancer hybrids. *European Journal of Medicinal Chemistry* 142:179–212. DOI: 10.1016/j.ejmech.2017.07.033.

Kraljević TG, Harej A, Sedić M, Pavelić SK, Stepanić V, Drenjančević D, Talapko J, Raić-Malić S. 2016. Synthesis, in vitro anticancer and antibacterial activities and in silico studies of new 4-substituted 1,2,3-triazole–coumarin hybrids. *European Journal of Medicinal Chemistry* 124:794–808. DOI: 10.1016/j.ejmech.2016.08.062.

Krištafor S, Bistrović A, Plavec J, Makuc D, Martinović T, Kraljević Pavelić S, Raić-Malić S. 2015. One-pot click synthesis of 1,2,3-triazole-embedded unsaturated uracil derivatives and hybrids of 1,5- and 2,5-disubstituted tetrazoles and pyrimidines. *Tetrahedron Letters* 56:1222–1228. DOI: 10.1016/j.tetlet.2015.01.152.

Kumar K, Sagar S, Esau L, Kaur M, Kumar V. 2012. Synthesis of novel 1H-1,2,3-triazole tethered C-5 substituted uracil-isatin conjugates and their cytotoxic evaluation. *European Journal of Medicinal Chemistry* 58:153–159. DOI: 10.1016/j.ejmech.2012.10.008.

Kusanur RA, Kulkarni M V., Kulkarni GM, Nayak SK, Guru Row TN, Ganesan K, Sund CM. 2010. Unusual anisotropic effects from 1,3-dipolar cycloadducts of 4-azidomethyl coumarins. *Journal of Heterocyclic Chemistry* 47:91–97. DOI: 10.1002/jhet.273.

Laco GS. 2011. Evaluation of Two Models for Human Topoisomerase I Interaction with dsDNA and Camptothecin Derivatives. *PLoS ONE* 6:e24314. DOI: 10.1371/journal.pone.0024314.

Li D-Z, Zhang Q-Z, Wang C-Y, Zhang Y-L, Li X-Y, Huang J-T, Liu H-Y, Fu Z-D, Song H-X, Lin J-P, Ji T-F, Pan X-D. 2017. Synthesis and antitumor activity of novel substituted uracil-1′(N)-acetic acid ester derivatives of 20(S)-camptothecins. *European Journal of Medicinal Chemistry* 125:1235–1246. DOI: 10.1016/j.ejmech.2016.11.013.

Lombardino JG, Lowe JA. 2004. The role of the medicinal chemist in drug discovery — then and now. *Nature Reviews Drug Discovery* 3:853–862. DOI: 10.1038/nrd1523.

Ma T, Ma Q-S, Yu B, Liu H-M. 2019. Discovery of the theobromine derivative MQS-14 that induces death of MGC-803 cells mainly through ROS-mediated mechanisms. *European Journal of Medicinal Chemistry* 174:76–86. DOI: 10.1016/j.ejmech.2019.04.044.

Melo NFS, Grillo R, Moraes CM, Brito CL, Trossini GHG, Menezes CMS, Ferreira EI, Rosa AH, Fraceto LF. 2007. Preparação e caracterização inicial de complexo de inclusão entre nitrofurazona e 2-hidroxipropil-β-ciclodextrina. *Revista de Ciencias Farmaceuticas Basica e Aplicada* 28:35–44.

Moraes MC, Lenardão EJ, Barcellos T. 2021. Synthesis of C4-substituted coumarins via Pechmann condensation catalyzed by sulfamic acid. Insights into the reaction mechanism by HRMS analysis. *Arkivoc* 2021:151–163. DOI: 10.24820/ark.5550190.p011.645.

Morris GM, Huey R, Lindstrom W, Sanner MF, Belew RK, Goodsell DS, Olson AJ. 2009. AutoDock4 and AutoDockTools4: Automated docking with selective receptor flexibility. *Journal of Computational Chemistry* 30:2785–2791. DOI: 10.1002/jcc.21256.

Naik RJ, Kulkarni M V., Sreedhara Ranganath Pai K, Nayak PG. 2012. Click Chemistry Approach for Bis-Chromenyl Triazole Hybrids and Their Antitubercular Activity. *Chemical Biology & Drug Design* 80:516–523. DOI: 10.1111/j.1747-0285.2012.01441.x.

Negrón-Silva GE, González-Olvera R, Angeles-Beltrán D, Maldonado-Carmona N, Espinoza-Vázquez A, Palomar-Pardavé ME, Romero-Romo MA, Santillan R. 2013. Synthesis of new 1,2,3-triazole derivatives of uracil and thymine with potential inhibitory activity against acidic corrosion of steels. *Molecules* 18:4613–4627. DOI: 10.3390/molecules18044613.

Peña-Morán OA, Villarreal ML, Álvarez-Berber L, Meneses-Acosta A, Rodríguez-López V. 2016. Cytotoxicity, post-treatment recovery, and selectivity analysis of naturally occurring podophyllotoxins from Bursera fagaroides var. fagaroides on breast cancer cell lines. *Molecules* 21:1–15. DOI: 10.3390/molecules21081013.

Pingaew R, Saekee A, Mandi P, Nantasenamat C, Prachayasittikul S, Ruchirawat S, Prachayasittikul V. 2014. Synthesis, biological evaluation and molecular docking of novel chalcone–coumarin hybrids as anticancer and antimalarial agents. *European Journal of Medicinal Chemistry* 85:65–76. DOI: 10.1016/j.ejmech.2014.07.087.

Popov Aleksandrov A, Mirkov I, Ninkov M, Mileusnic D, Demenesku J, Subota V, Kataranovski D, Kataranovski M. 2018. Effects of warfarin on biological processes other than haemostasis: A review. *Food and Chemical Toxicology* 113:19–32. DOI: 10.1016/j.fct.2018.01.019.

Reddy DS, Hosamani KM, Devarajegowda HC. 2015. Design, synthesis of benzocoumarin-pyrimidine hybrids as novel class of antitubercular agents, their DNA cleavage and X-ray studies. *European Journal of Medicinal Chemistry* 101:705–715. DOI: 10.1016/j.ejmech.2015.06.056.

Salar U, Khan KM, Jabeen A, Faheem A, Fakhri MI, Saad SM, Perveen S, Taha M, Hameed A. 2016. Coumarin sulfonates: As potential leads for ROS inhibition. *Bioorganic Chemistry*

69:37–47. DOI: 10.1016/j.bioorg.2016.09.006.

Sander T, Freyss J, von Korff M, Reich JR, Rufener C. 2009. OSIRIS, an Entirely in-House Developed Drug Discovery Informatics System. *Journal of Chemical Information and Modeling* 49:232–246. DOI: 10.1021/ci800305f.

Sandhu S, Bansal Y, Silakari O, Bansal G. 2014. Coumarin hybrids as novel therapeutic agents. *Bioorganic and Medicinal Chemistry* 22:3806–3814. DOI: 10.1016/j.bmc.2014.05.032.

Saokham P, Muankaew C, Jansook P, Loftsson T. 2018. Solubility of cyclodextrins and drug/cyclodextrin complexes. *Molecules* 23:1–15. DOI: 10.3390/molecules23051161.

Shalini, Kumar V. 2021. Have molecular hybrids delivered effective anti-cancer treatments and what should future drug discovery focus on? *Expert Opinion on Drug Discovery*:1–29. DOI: 10.1080/17460441.2021.1850686.

Shalini K, Kumar N, Drabu S, Sharma PK. 2011. Advances in synthetic approach to and antifungal activity of triazoles. *Beilstein Journal of Organic Chemistry* 7:668–677. DOI: 10.3762/bjoc.7.79.

Simijonović D, Vlachou EE, Petrović ZD, Hadjipavlou-Litina DJ, Litinas KE, Stanković N, Mihović N, Mladenović MP. 2018. Dicoumarol derivatives: Green synthesis and molecular modelling studies of their anti-LOX activity. *Bioorganic Chemistry* 80:741–752. DOI: 10.1016/j.bioorg.2018.07.021.

Singh H, Singh JV, Bhagat K, Gulati HK, Sanduja M, Kumar N, Kinarivala N, Sharma S. 2019. Rational approaches, design strategies, structure activity relationship and mechanistic insights for therapeutic coumarin hybrids. *Bioorganic and Medicinal Chemistry* 27:3477–3510. DOI: 10.1016/j.bmc.2019.06.033.

Spartan ’08, Version 1.2.0; Wavefunction, Inc.; Irvine, CA 92612, USA 2008. No Title.

Staker BL, Hjerrild K, Feese MD, Behnke CA, Burgin AB, Stewart L. 2002. Nonlinear partial differential equations and applications: The mechanism of topoisomerase I poisoning by a camptothecin analog. *Proceedings of the National Academy of Sciences* 99:15387–15392. DOI: 10.1073/pnas.242259599.

Thakur A, Singla R, Jaitak V. 2015. Coumarins as anticancer agents: A review on synthetic strategies, mechanism of action and SAR studies. *European Journal of Medicinal Chemistry* 101:476–495. DOI: 10.1016/j.ejmech.2015.07.010.

Torres FC, Gonçalves GA, Vanzolini KL, Merlo AA, Gauer B, Holzschuh M, Andrade S,

Piedade M, Garcia SC, Carvalho I, Poser GL von, Kawano DF, Eifler-Lima VL, Cass QB. 2016. Combining the Pharmacophore Features of Coumarins and 1,4-Substituted 1,2,3-Triazoles to Design New Acetylcholinesterase Inhibitors: Fast and Easy Generation of 4-Methylcoumarins/1,2,3-triazoles Conjugates via Click Chemistry. *Journal of the Brazilian Chemical Society* 27:1541–1550. DOI: 10.5935/0103-5053.20160033.

Xu X, Wu Y, Liu W, Sheng C, Yao J, Dong G, Fang K, Li J, Yu Z, Min X, Zhang H, Miao Z, Zhang W. 2016. Discovery of 7-Methyl-10-Hydroxyhomocamptothecins with 1,2,3-Triazole Moiety as Potent Topoisomerase I Inhibitors. *Chemical Biology & Drug Design* 88:398–403. DOI: 10.1111/cbdd.12767.

Xu Z, Zhao S-J, Liu Y. 2019. 1,2,3-Triazole-containing hybrids as potential anticancer agents: Current developments, action mechanisms and structure-activity relationships. *European Journal of Medicinal Chemistry* 183:111700. DOI: 10.1016/j.ejmech.2019.111700.

Yang JM, Chen CC. 2004. GEMDOCK: A Generic Evolutionary Method for Molecular Docking. *Proteins: Structure, Function and Genetics* 55:288–304. DOI: 10.1002/prot.20035.

Ye XW, Zheng YC, Duan YC, Wang MM, Yu B, Ren JL, Ma JL, Zhang E, Liu HM. 2014. Synthesis and biological evaluation of coumarin-1,2,3-triazole- dithiocarbamate hybrids as potent LSD1 inhibitors. *MedChemComm* 5:650–654. DOI: 10.1039/c4md00031e.

Zhang L, Xu Z. 2019. Coumarin-containing hybrids and their anticancer activities. *European Journal of Medicinal Chemistry* 181:111587. DOI: 10.1016/j.ejmech.2019.111587.